ACADEMIA ROMÂNĂ
Revue Roumaine de Chimie
https://web.icf.ro/rrch/

Rev. Roum. Chim.,
2022, *67*(10–12), 525–534
DOI: 10.33224/rrch.2022.67.10-12.02

AN INVESTIGATION INTO SYNTHESIS AND CHARACTERIZATION OF Ag-NANOPARTICLES USING GREEN CHEMISTRY, AND THEIR ANTIBACTERIAL PROPERTIES

M. Mazhar Abbas SHAHANI,[a] Farzana AHMAD,[b,*] Muhammad JAMIL[e] and Musa Kaleem BALOCH[c,d,*]

[a] Department of Chemistry, University of Sargodha, Sargodha, Punjab, Pakistan
[b] Department of Chemistry, Konkuk University, Seoul 05029, Korea
[c] Institute of Chemical Science, Department of Chemistry, Gomal University, D. I. Khan, Pakistan
[d] Department of Chemical & Life Sciences, Qurtuba University of Science & Information Technology, D. I. Khan, Pakistan
[e] Sang-Ho College & Department of Physics, Konkuk University, Seoul 05029, Korea

Received April 8, 2022

The quest for new nano-systems is ongoing to provide tailored nanoparticle systems for commercial purposes. The ability to manage their size and morphology leads to an advantage over other characteristics, therefore, a stable generation system is considered critical for their applications. We employed rose plant leaves extract to generate Ag-NPs via silver nitrate ($AgNO_3$) as a basic ingredient in this study. The procedure was executed for multiple concentrations of the plant extract, as well as varying amounts of salt, and for different time periods. All of the different steps resulted in the development of Ag-NPs. The emergence of an absorption peak at 425 nm in UV-Vis spectroscopic spectra, and the presence of spherical particles visualized through SEM provided evidence of the creation of small-sized Ag-NPs. Finally, using the spread plate method, the antibacterial activity of Ag-NPs was investigated, and it was discovered that Ag-NPs exhibit high antibacterial activity against the four bacterial strains.

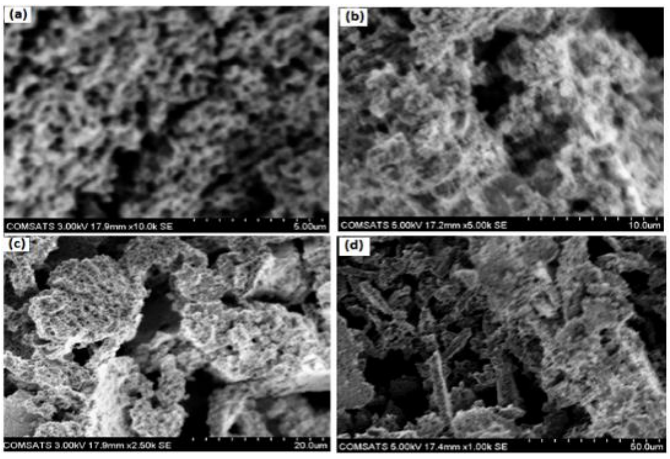

INTRODUCTION

Nanoparticles research is currently a hot topic among the scientific community due to its wide range of possible applications in almost every aspect of our lives.[1] The motivation behind why nanoparticles (NPs) are appealing for almost every application depends on their vital and remarkable characteristics, for instance, their surface area to mass ratio, which is much larger than that of various particles and materials, taking into account synergistic advancement of responses, and additionally, their very high capacity to absorb and the increase the reactivity of the surface serving vehicle or as a carriage for different compounds.[1,2] Among them, Ag-NPs (nano-silver) have sparked particular interest due to their superior physical and chemical capabilities as compared to their counterparts. These offer various properties including high electrical and thermal conductivity, surface-enhanced Raman scattering, compound steadiness, synergist movement and non-direct

* Corresponding author: farzana@konkuk.ac.kr, musakaleem2001@yahoo.com

optical conducts.[3] Ag-NPs also exhibit a broad range of bioactivities including bactericidal and fungicidal properties. Currently, nano-silver is being used commercially in a wide range of industrial, and common materials *e.g*., consumer-based household items including garments, furniture, electronic items, ladies' makeup kits, kids' toys, plastics, cleansers and glues, leading to an increase in their shelf life.[4] It is believed that Ag-NPs' negative effects are insignificant or nonexistent. Ag-NPs are additionally utilized in the medicinal field as an indispensable material both in surgical and non-surgical items, for example, wound dressings, gauzes, catheters and so forth.[5]

By definition, "Green Chemistry" or "Sustainable Chemistry" is the design of chemical products and processes that limit or avoid the use or production of hazardous substances.[6,7] At present, the growing interest in biological systems that do not employ toxic chemicals as by-products stems from the need for environmentally non-toxic synthetic methods for nanoparticles' manufacturing. As a result, there is a growing trend of research interests in the field of "green nanotechnology".[8-10] Furthermore, many biological methodologies for nanoparticle synthesis have been extensively reported using plants and microorganisms such as bacteria, and fungi, as these are biologically safe, cost-effective, and environment-friendly. However, at present, the most widely used way of producing green, or eco-friendly nanoparticles is the fabrication of nanoparticles utilizing plant extracts as plants provide a better platform for nanoparticles synthesis as most of them are free of toxic chemicals as well as provide natural capping agents.[9,10] Additionally, plants are widely dispersed, conveniently accessible, and safer to work with and most of them are bioactive and can enhance the activity of particles.[10-12]

Over the past few years, intensive studies have been performed on novel green synthesis for the nanoparticles including metal and metal oxides-based nanoparticles with their applications in various medical fields including cancer,[12-16] Silver, gold and magnetite nanoparticles-based works,[13] metal nanoparticle from natural extracts of plants or their metabolites.[14] Because of its quick, eco-friendly, non-pathogenic, affordable protocol and provision of a single-step approach for biosynthetic processes, the use of plants as a production assembly of Ag-NPs has piqued the interest of researchers.[17] Further, Ag-NPs are synthesized by utilizing biological mechanisms, which are thought to be preferable since AgNPs are fabricated without the use of any harsh, toxic, or costly chemical ingredients.[18-20]

Rosa indica (Rose) is a rosa genus perennial floral shrub.[21] It is a member of the *Rosaceae* family, which includes rhizomatous, thorny, or climbing plants, shrubs, and trees.[21,22-24] Various rose compositions are employed in Indian medicine as an astringent, tonic, mild laxative, and antibacterial agent, as well as in the treatment of sore throat, swollen tonsils, and gall stones, for cooling effect, and as a carrier for other medications.[25] *Rose damascena* essential oil is thought to have anti-inflammatory and anti-spasmodic properties.[26] Further rose extract and its isolates have been shown to have antibacterial, anti-HIV, and hypnotic effects.[27-29] Rose oil has also been shown to have a favorable influence on a variety of digestive system diseases when consumed as food.[23]

In the present scenario, we have considered rosa indica plants for the current work. To our knowledge, both of such plants have not been investigated to synthesize the A-NPs via leaf extracts of rosa indica plants. The objective of the current investigation is the production of Ag-NPs utilizing green chemistry (rose leaves extract) and improvements in biosynthetic procedures. The impact of the amount of concentrate, substrate fixation, temperature, and pH on the morphology of Ag-NPs was considered. The morphological characterization of AgNPs was performed using latest available techniques including scanning electron microscope (SEM). To investigate the bioactivity of the synthesized nanoparticles for various bacterial strains, a proper technique was employed so that the material can be utilized for medical applications.

EXPERIMENTAL

Materials and methods

For the synthesis and characterization of Ag-NPs, as well as for the extraction of rose leaves, analytical standards and pure chemicals were used. The Whatman filter paper,[30] distilled and deionized water were purchased from the local market (Lahore, Pakistan).

Silver nitrates ($AgNO_3$), nutrient broth, nutrient agar were of Analytical grade acquired from Hi media. Four bacterial strains *e.g., Escherichia coli*,[31] *Staphylococcus aureus*,[32] *Salmonella Typhi*[33] and *Pseudomonas aeroginosa*[34] used in this study were obtained from Lahore, Punjab (Pakistan). All other compounds were obtained from E. Merck, Germany.

Preparation of plant extracts

The synthesis and characterization of Ag-NPs were carried out at Star Laboratories in Lahore, Punjab, Pakistan. The fresh leaves of rosa indica[21] were collected from Lahore, Pakistan, and were washed properly with water to remove dust particles and after that they were dried under the sun and crushed into a fine powder.

Immediately after that, the plant extracts in water were made by combining 10 percent powder with deionized water in a 250 mL conical flask. The mixture was then incubated for 30 minutes before being centrifuged at 5,000 rpm for 30 minutes at room temperature.

The supernatant was removed and filtered using a vacuum filter and 1 mm pore-size filter. The extracts were collected and stored at room temperature about 15 minutes for additional investigations. The details of the adjusted parameters are provided in Table 1.

Table 1

Preparation parameters for leave extracts

Plants	Weight (gm)	Volume of deionized water (mL)	Temperature (^{0}C)	Stirring duration (min)	Centrifugation time @ 5,000 rpm (min)
Rose leaves	10	100	100	30	30

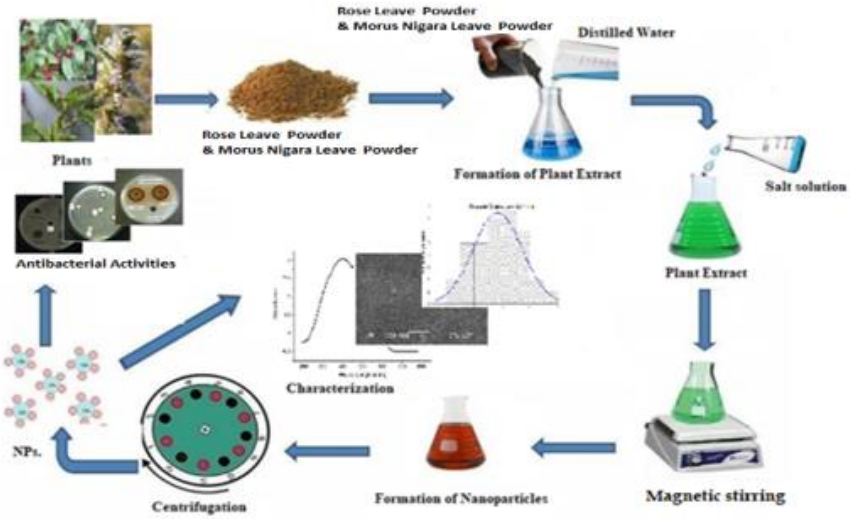

Fig. 1 – Green chemistry synthetic technique for the development of Ag-NPs adopted in the current work. The figure has been adopted from Ref. [20] in its modified form.

Table 2

Parameters for the synthesis of silver nanoparticles using leave extracts and silver nitrate solution

Sample #	Vol. (mL) of $AgNO_3$ (1 mM) solution used	Volume (mL) of extract used	Time (h) of reaction	Temperature (^{o}C)	Centrifugation (5,000 rpm) time (min)
1	50	5	1	90	30
2	150	15	1	90	30
3	150	50	1	90	30
4	150	100	120	30	30

Synthesis of Ag nanoparticles

Freshly prepared plant extracts and a solution of $AgNO_3$ were prepared. The synthetic procedure of pure Ag-NPs using leaves and silver nitrate solution can be seen in Table 2, while the proposed green synthetic technique can be observed in Fig. 1. In a 250 mL beaker with 100 ml deionized water, a 1 mM solution of $AgNO_3$ was produced. 5 mL of leaf extract was combined with 50 mL of a 1 mM $AgNO_3$ solution. For one hour, the mixture was heated to 90 ^{o}C for the conversion of Ag^+ to Ag-NPs.[10] In this case, the leave extract worked as a reducing and stabilizing material for the particles.

As nanoparticles exhibit optical properties that are sensitive to size, shape, concentration, aggregation state, and refractive index near the nanoparticle's surface, UV/visible spectroscopy (UV-Vis) is a helpful technique for detecting, characterizing, and analyzing these materials. Nanoparticles formed of certain materials, such as gold and silver, interact

strongly with specific wavelengths of light, and the distinctive optical proportion of these materials serves as a basis for the field of plasmonics. As a result, the UV-Vis spectra were recorded for the bio-reducing aqueous solution of extract and $AgNO_3$. For the purpose the measurements, tests were made in the range of 360 to 600 nm wavelength. The recorded spectra indicated the formation of Ag-NPs.

Scanning electron micrsoscope (SEM) analysis

The scanning electron microscope (SEM) slides were made by smearing the solutions with the developed Ag-NPs from leave extracts after 24 h of $AgNO_3$ injection. To make the samples conductive, a small layer of platinum was applied. The samples were then analyzed through the SEM (JSM-5910LV) at a 20 KV accelerating voltage.

Antibacterial activity test

Muller Hinton Agar Media (1 L)[35] was made by combining 33.9 g of commercially available Muller Hinton Agar Medium (HiMedia) with 1,000 mL of distilled water. The dissolved media was autoclaved for 15 min at 15 lbs pressure and 121°C. To achieve a uniform microorganism suspension in terms of bacteria, the microorganism suspension was thoroughly mixed. A sterilized wire lope was dipped into the suspension to extract the required amount of suspension and inoculated in the sterilized media, ensuring that the temperature of the media did not exceed 50ºC, shaken well, and 20 mL of this incubated media was poured into each Petri plate (sterilized at 160 ºC for one and a half hour), allowing it to jolly.

It was ensured that all of these activities took place in a Laminar air flow (LAF) cabinet that met USP customary class 100 (class A) standards, had a differential pressure of not less than 0.05 in of water column or 12 Pa, and air changes of not less than 100/h. The bioburden was kept at less than 1 cfu. With a sterilized borer, wells were dug in Petri dishes containing 20 mL of Muller Hinton media that had been seeded with a 24 h culture of bacterial strains, and each well was filled with 20 L of the nanoparticles. The plates were then incubated for 24 h at 37 °C.

Agar well diffusion method

The Agar well diffusion method was used to test the effect of Ag-NPs on bacterial strains. The nanoparticles were permitted to diffuse into the media and communicate with the test organisms in a freshly seeded plate. Because of the confluent lawn of growth, the resulting zones of inhibition were homogeneously circular. The zone of inhibition's diameter was taken in mm. As a part of the current investigations, fluid concentrate (hostile to bacterial action) which was dictated by well dissemination technique for the selected four bacterial strains[31-34] were utilized for this purpose. This culture was developed by spread plate strategy. Gentamycin circle was used as a standard control; also deionized water was used as a control for the concentrate. The plates were then hatched for 24 h at 37 °C. To investigate the growth of microorganisms in stock culture, 5 mL of bacterial culture was placed in a 250 mL carafe, encasing 200 mL of bacteria nutrient agar.

Following the above step, we circulated the sample plates in in a lab-line hatchery shaker at 37 °C and was shaken at 175 rpm for 24 h. A mixture with ratio of 1:10 with 24 h bacterial development and sterilized physiological saline water was prepared. 100 µL of each arrangement was placed in different wells of the Bioscreen C. The main segment wells served as controls and lacked in Ag-NPs. Aliquots of 10 L and 20 L of various Ag-NP convergences were added to the samples. The rate of development was determined by measuring turbidity with the Bioscreen C for a total of 24 h at regular intervals of 15 min. With the end goal of determining the bio-medicinal impact of Ag-NPs in mind, Gram-positive and Gram-negative microscopic organisms were exposed to two distinct groups of Ag-NPs (2 ppm and 4 ppm). Based on the turbidity estimation over a 24 h period, an optical density thickness band was developed. Such estimation was then used to generate microbiological development bands that plotted turbidity versus time.

RESULTS AND DISCUSSION

Visual observations and UV-Vis spectroscopy

The reduction of silver ions into Ag-NPs was observed as a result of color change during exposure to plant extracts.[10] The color shift was caused by surface plasmon resonance (SPR). Due to combined vibrations of metal nanoparticle electrons in resonance with a light wave, metal nanoparticles have free electrons, which results in the SPR absorption band. The intensity of the absorption peak increased with an increase in time. The color variations in the characteristic bands were caused by the excitation of the SPR in the Ag-NPs. UV-Vis spectroscopy can be used to study the amount of strain in atoms. The changes in the spectra due to angular distortion can correlate with the amount of conjugation in strained atoms. It can also be used to distinguish tautomeric forms. It was demonstrated that the solution's UV-Vis spectrum is complementary to its extra-abundant tautomers.

The production of Ag-NPs by biosynthesis using rose leaves extract was confirmed using a UV-Vis spectrophotometer. The absorption spectra are plotted against wavelength from 200 to 800 nm in Fig. 2. The bands for Ag-NPs are stable and produced by SPR, which appeared around 425 nm, which is roughly in the range for the absorption spectra of the synthesized silver nanoparticles.[10] As shown in Fig. 3, the spectra were measured as a function of reaction time as soon as the rose leaves extract and silver nitrate were mixed, and were used to record the formation of silver ions.

The spectra above show that as reaction time passes, the number and size of the Ag-NPs increase. The broadness of the spectrum and the shift in the absorbance peak indicate that the Ag-NPs require time to settle, which implies that the reaction takes a while to complete. In terms of particle size, it has been observed visually that their size increases slightly in comparison to the initial stage of the reaction when the extract is mixed with the salt.

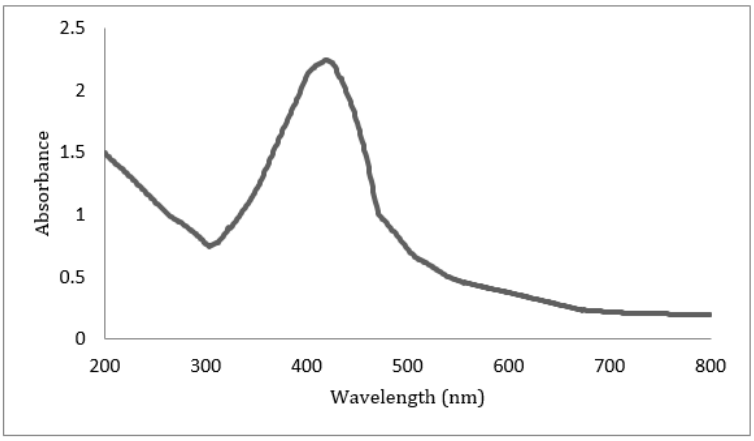

Fig. 2 – UV-Vis spectra for the silver nanoparticles.

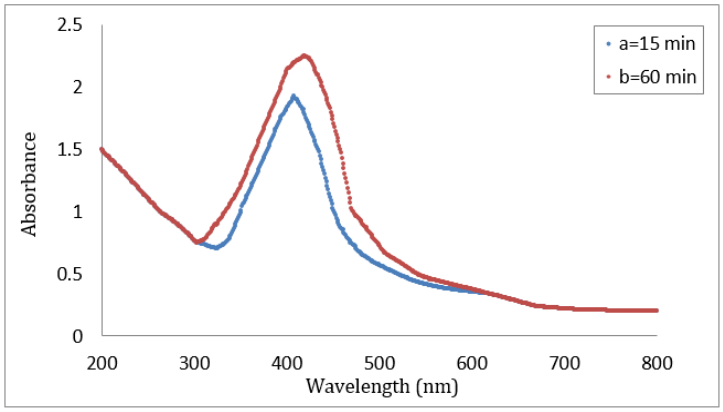

Fig. 3 – UV-Vis spectra for the silver nanoparticles resulted from the mixing of the rose leaves extract in $AgNO_3$ solution.

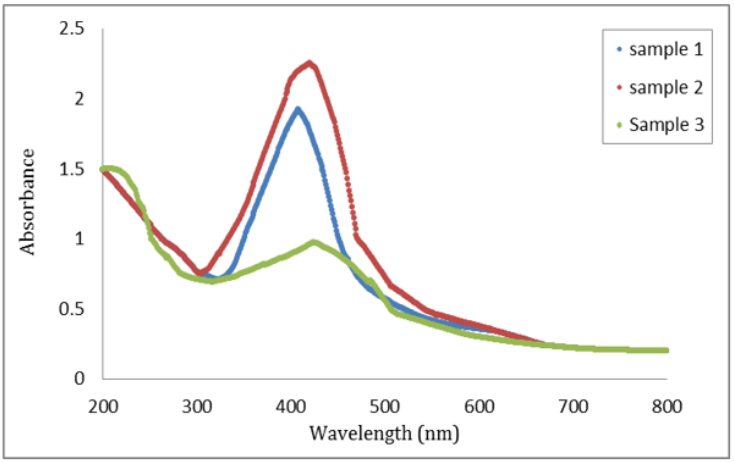

Fig. 4 – UV-Vis spectra for the three samples obtained by the same synthetic procedure adopted for the first sample.

Furthermore, the synthetic procedure was repeated for the other three additional samples, and the spectral data plotted in Fig. 3 shows that very similar types of Ag-NPs were again produced. Although the reaction time treatment was not used in this case, Fig. 4 shows very similar behavior as observed for the first sample. Based on the absorbance spectrum data, we can conclude that the synthesized Ag-NPs are nearly spherical in shape.

Structural and morphological analysis using scanning electron microscopy (SEM)

SEM was utilized extensively in this study to analyze all samples containing Ag-NPs generated from varied concentrations of the $AgNO_3$ salt employed.

a) Sample 1

The first of these samples was prepared by combining 50 ml of $AgNO_3$ solution (1 mM) in 100 ml deionized water with 5 mL of sample. The rose leaves extract comprised 10 g of rose leaves in 100 mL of deionized water. Figures 5–7 show the SEM micrographs acquired for this material. The micrographs of Ag-NPs (sample 1), display the electric stub into which the wet and dry nanoparticles were inserted (can be observed in Fig. 5).

A clear and distinct production of Ag-NPs can be seen in the SEM micrographs. The particle size, on the other hand, appears to fluctuate. It is worth noting that extremely tiny nanoparticles appear separately, as well as a large cluster of particles. The likely reason for such a wide variety of sizes is that the drying process of Ag-NPs was inadequate, causing tiny-sized particles to stick together, resulting in massive agglomerates of Ag NPs, which appeared as enormous clumps throughout. The earlier reports[17,18,20] also show comparable behavior for Ag-NPs. It has also been observed that agglomerates may form as a result of the utilized concentrated electron beam.[17,18,20] The histogram of the Ag-NPs calculated is depicted in Fig. 8, revealing a mean size of around 100 nm diameter particles.

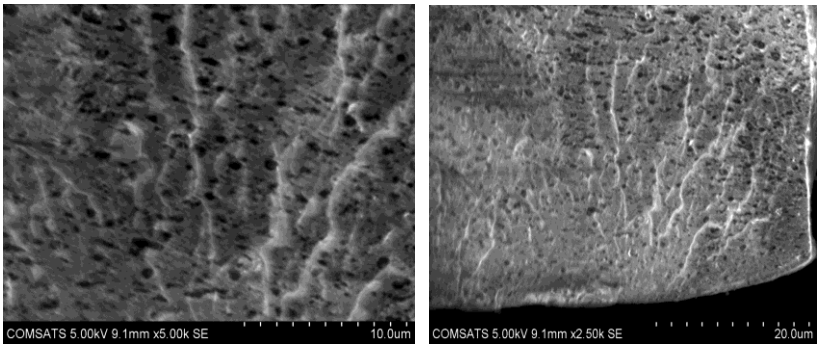

Figs. 5–6 – SEM image of Ag-NPs (Sample 1) with gradually increase in the voltage of focused beam of electrons, the below micrograph with higher magnification roughly indicates the size of the silver nanoparticles.

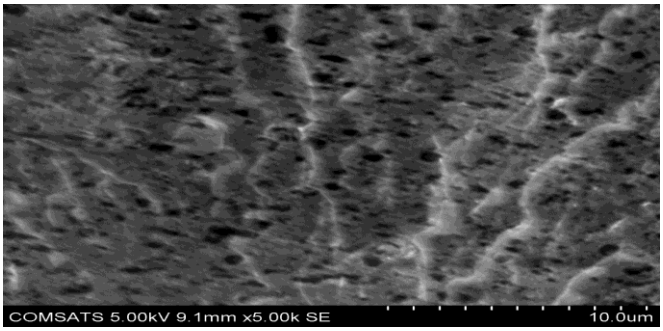

Fig. 7 – Additional SEM image of Ag-NPs (sample 1). Detailed look suggests a range of size distribution of the nanoparticles with medium size of approximate 40 nm for the smallest particles and for the larger one approaches around 400 nm.

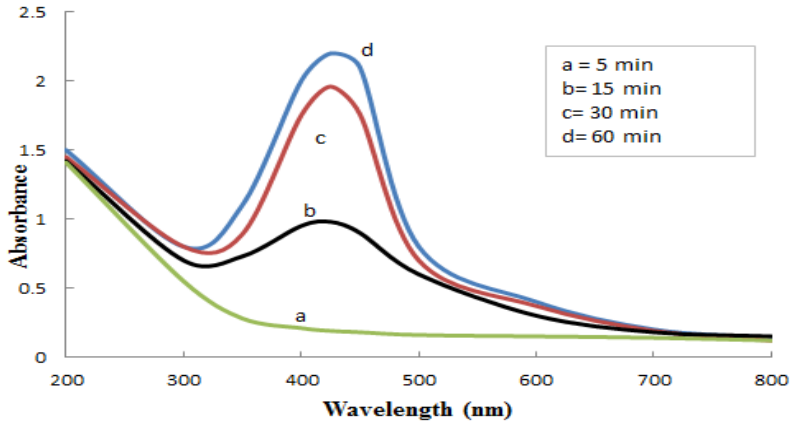

Fig. 8 – Histogram of Ag-NPs (Sample 1) showing the Absorbance Vs Wavelength spectra.

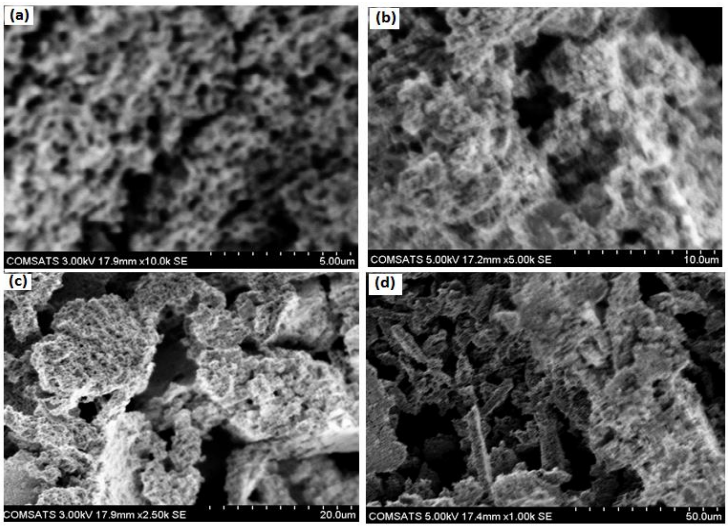

Fig. 9 – SEM images of silver nanoparticles obtained from: (a–b, c) pure AgNPs, (d) 50 mL $AgNO_3$ mixed with 5 mL silver nitrate solution extract. It clearly indicates the formation of agglomerates of small nanoparticles whose size in comparison to previous sample is assumed to be 40 nm at least.

b) Sample 2

Another effort was undertaken to synthesize Ag-NPs using the same rose leaves extract and silver nitrate solution as in the previous case, but with a little variation in the plant extract preparation process. Fig. 9(a–d) depict SEM micrographs of the current samples with increasing magnification. The approach used to generate Ag-NPs was repeated for another material, and it was proven through analysis of SEM micrographs that we successfully developed Ag-NPs. The percentage of agglomeration appears to be higher, which is not matching with the proportion of salt combined in the leaf extract; rather, it might be due to the sample not highly dried. This assertion seems reasonable since the white crisp fringes shown in many micrographs are caused by water.

The morphology of such a nano-system is challenging since visualizing a single particle is not easy; nevertheless, a detailed examination of the data reveals the round form of the Ag-NPs, as was the case for our first sample.

c) Sample 3

This time, the proportions of sample rose leaf extract and standard rose leaves (~wt: 10g) solution were compared to see if a change in the percentage of the mixture affected the overall composition, size, structure, and morphology of the Ag-NPs generated. When a pure 150 mL silver salt and 15 mL extract of the leaves were combined, the ratio of standard leaves to sample leaves was 10 times greater. It produced a combination of nanoparticles with a homogeneous formation but an increased number of particles (can be seen in Fig. 10).

It can be observed that a larger proportion of $AgNO_3$ solution as compared to sample leaves results in a completely different outcome with no apparent clarity of particle size and morphology but rather a uniform distribution with a high chance of the particles being of the same size. A high-quality SEM micrograph may be useful to confirm the pivotal role performed by either the silver nitrate solution or the proportion of sample leaves.

d) Sample 4

In this case, the process was repeated and verified in proportion to the reaction time. When the leaf extract is combined with the $AgNO_3$, the mixture is normally heated for a short period of time to speed up the reaction and stirred as well. For this sample, however, 150 mL of standard leaves were combined with 50 ml of sample leaves in a 3:1 ratio and kept for two weeks without any heating or stirring.

It was discovered that very beautiful and symmetrical Ag-NPs, as shown in Fig. 11, were fabricated. The resulting Ag-NPs had a very narrow size distribution, and the approximate size of a single nanoparticle was about 30 nm, which was slightly smaller than previously discovered; nevertheless, the estimate was not particularly exact. Here, once again, agglomeration was

detected similar to those in other samples. As the material scanned was highly concentrated, this might have resulted in agglomerates of Ag-NPs in practically every sample.

All of the Ag-NPs samples generated in this study show a clear image of rose leaves extract being mixed with silver nitrate salt effectively resulting in the creation of tiny-sized Ag-NPs with virtually spherical /round morphology.

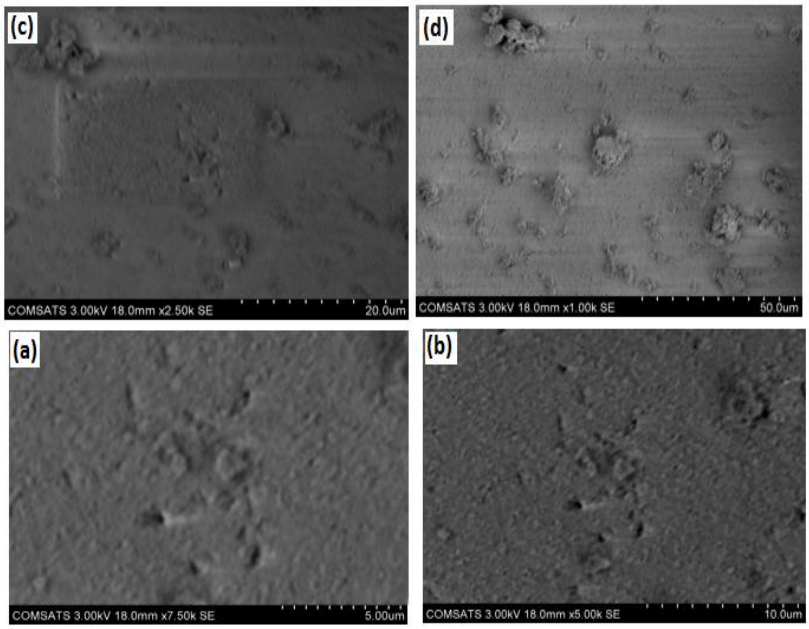

Fig. 10 – Solution mixed with 15 mL rose sample leaves extract SEM images for pure Ag NPs produced from 150 mL silver nitrate. The images are shown with increase in magnification and smaller scale bar. No prominent size of nanoparticles is possible to be estimated.

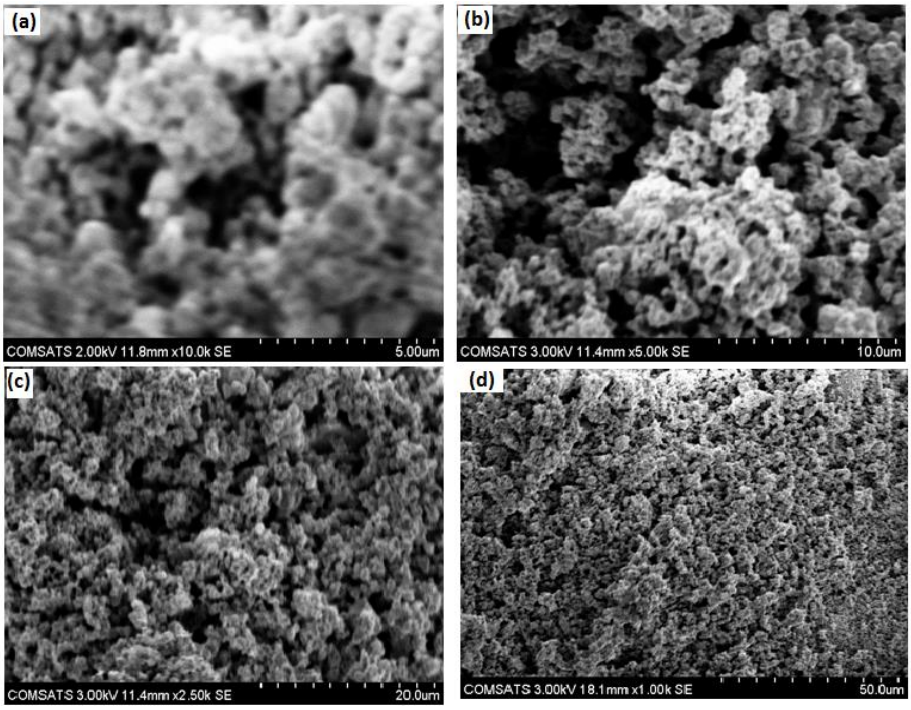

Fig. 11 – Micrographs of pure sample of silver nanoparticles (a–d): In this sample the proportion of salt and extract remains 150 and 50 mL each. The size of Ag NPs in this case appears to be small around 30 nm as compared with other samples, but visualization of individual particles is not possible due to large amount of sample present.

Table 3

Observation of zone of inhibition of *Staphylococcus aureus*

Staphylococcus Aureus	**Concentration of AgNPs (µg/mL)**	**Zone of inhibition**
	20	04 mm
	40	06 mm
	60	10 mm
	80	16 mm
Escherichia Coli	20	No Zone
	40	No Zone
	60	No Zone
	80	No Zone
Pseudomonas Aeroginosa	20	No Zone
	40	No Zone
	60	No Zone
	80	No Zone
Salmonella Taphi	20	No Zone
	40	No Zone
	60	No Zone
	80	No Zone

Anti-bacterial activity test results

The antibacterial activity was determined by using Vernier Caliper to measure the diameter of the inhibition zone generated around the well. Except for *Staphylococcus aureus*, no inhibitory zone was detected for the remaining three bacterial strains *e.g. E. coli*, *Salmonella typhi* and *Pseudomonas aeruginosa.*

Measurement of zone of inhibition

The zone of inhibition demonstrated the antibacterial activity of Ag-NPs, as shown in Table 3. The result revealed that the antimicrobial activity of Ag-NPs is concentration-dependent; as the concentration of Ag-NPs increases, so does the zone of antimicrobial activity.

While in the case of staphylococcus aureus, very prominent inhibition zones were observed. With 20, 40, 60, and 80 µg/mL of Ag-NPs concentrations, clear inhibitions were showed, with less concentration resulting in a smaller inhibition zone and higher concentration resulting in a larger inhibition zone, ensuring the effectiveness of Ag-NPs antibacterial activity against *Staphylococcus aureus*. Such inhibition scenarios can be observed in Fig. 12.

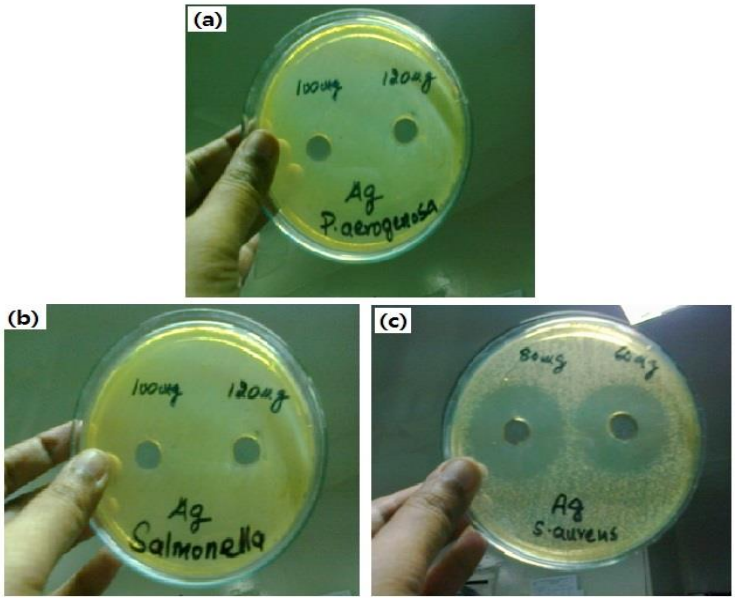

Fig. 12 – Zone of inhibition of (a) *Pseudomonas aeruginosa* (b) *Salmonella Taphi* and (c) *Staphylococcus aureus*.

CONCLUSIONS

The Ag-NP particles were prepared utilizing the green method. Ag-NPs were effectively produced using leaves extracts. The required nanoparticles were fabricated by combining rose leaves extract with $AgNO_3$ solution for bio-reduction. It was discovered that the quantities of the salt and extract had a significant impact on the size and number of Ag-NPs generated.

UV-Vis spectroscopy was employed to investigate the surface plasmon resonance property of produced Ag-NPs, and the maximum band was discovered to be at 425 nm. The morphological analysis of Ag-NPs by SEM predicted that the nanoparticles were spherical in shape with their diameters between 450 nm to 1,000 nm in the range.

Furthermore, the antibacterial activity of Ag-NPs was determined to be significant against *Staphylococcus aureus*, with less activity against *Salmonella*, *Pseudomonas aeruginosa*, and *E-coli*. Ag-NPs showed higher activity as compared to a standard drug, Norfloxacin. Extensive research is needed in this subject to explore diverse applications of Ag-NPs that can be designed using this process.

REFERENCES

1. G. Zhao and S. E. Stevens Jr, *Biometals*, **1998**, *11*, 27.
2. J. Lemcke, F. Depner and U. Meier, *Acta Neurochir. Suppl.*, **2012**, *114*, 347.
3. B. G. Ershov, E. Janata, E. Henglein and A. Fojtlk, Unpublished report 2007.
4. C. Buzea, I. Pacheco and K. Robbie, *Bio. Inter. Phases*., **2007**, 2(4), MR17-MR71
5. Z.-J. Jiang, C.-Y. Liu and L.-W. Sun, *J. Phys. Chem. B*, **2005**, *109*, 1730.
6. P. J. Dunn, *Chem. Soc. Rev.*, **2012**, *41*, 1452.
7. https://www.epa.gov/greenchemistry/benefits-green-chemistry (last accessed 17th January, 2022).
8. B. Singhal, K. Kasariya, A. R. Sharma and R. P. Singh, *J. Nanopart. Res.*, **2011**, *13*, 2981.
9. P. Mukherjee, D. S. Mandal, S. Senapati, R. Sainkar, M. I. Khan, R. Parishcha, P. V. Ajaykumar, M. Alam, R. Kumar and M. Sastry, *Nano Lett.*, **2001**, *1*, 515.
10. G. Ghoshal and M. Singh, *Mater. Sci. Energ. Techn*., 2022, *5*, 22.
11. Y. Vitta, M. Figueroa, M. Calderon and C. Ciangherotti, *Mat. Sci. Energy Technol.*, **2020**, *3*, 97.
12. D. Zhang, X.-L. Ma, Y. Gu, H. Huang and G.-W. Zhang, *Front. in Chem.*, **2020**, *8*, 799.
13. P. Malik, R. Shankar, V. Malik, N. Sharma and T. K. Mukherjee, *J. Nano Part*., **2014**, 302429.
14. H. R. El-Seedi, R. M. El-Shabasy, S. A. M. Khalifa, A. Saeed, A. Shah, R. Shah, F. J. Iftikhar, M. M. Abdel-Daim, A. F. Omri, N. H. Hajrahand, J. S. M. Sabir, X. Zou, M. F. Halabi, W. Sarhann and W. Guo, *ASC Adv.*, **2019**, *9*, 24539.
15. N. Shreyash, S. Bajpai, M. A. Khan, Y. Vijay, S. K. Tiwary and M. Sonker, *ACS Appl. Nano Mater.*, **2021**, *4*, 11428.
16. A. Gour and N. K. Jain, *Nanomed. Biotech.*, **2019**, *47*, 844.
17. S. Ahmed, M. Ahmad, B. L. Swami and S. Ikram, *J. Advanced. Res*., **2016**, *7*, 17.
18. A. Ahmad, P. Mukherjee, S. Senapati, D. Mandal, M. Khan, R. Kumar and M. Sastry, *Coll. and Surf. B: Bio-interfaces*, **2003**, *28*, 313.
19. B. Ankamwar, C. Damle, A. Ahmad and M. Sastry, *J. NanoSci. Nanotech*., **2005**, *5*, 1665.
20. K. Mehdi, "Plant mediated metallic nanoparticles, synthesis and applications", *PhD thesis*, submitted to HEC, Islamabad, **2020**.
21. H. M. Rasheed, T. Khan, F. Wahid, R. Khan and A. J. Shah, *Evid.-Based Complem. and Alter. Med*., 2015, 279247.
22. W. L. Crepet, K. C. Nixon and M. A. Gandolfo, *Am. J. Bot*., **2004**, *91*, 1666.
23. W. Judd, C. Campbell, E. Kellogg, P. Stevens and M. Donoghue, "Plant Systematics: A Phylogenetic Approach", Sinauer Associates, Sunderland, Mass, USA, **1999**.
24. S. Bai, L. Seasotiya, A. Malik, P. Bharti and S. Dalal, *Der Pharmacia Lett*., **2015**, *7*, 179.
25. V. Singh, V. K. Kaul, B. Singh and R. P. Sood, "Supplement to Cultivation & Utilization of Aromatic Plants", S. S. Handa and M. K. Kaul (Eds.), RRL, Jammu Tawi, India, 1997, p. 195.
26. H. Sadraei, G. Asghari and S. Emami, *Research Pharma. Sci.*, **2013**, *8*, 17.
27. E. Basim and H. Basim, *Fitoterapia*, **2003**, *74*, 394.
28. E. S. Karthy, P. Ranjitha and A. Mohankumar, *Int. J. Bio*., **2009**, *1*, 34.
29. M. H. Boskabady, M. N. Shafei, Z. Saberi and S. Amini, *Iran. J. Basic Med. Sci*., **2011**, *14*, 295
30. Whatman filter paper: https://www.cytivalifesciences.com/en/us/shop/whatman-laboratory- filtration
31. O. Tenaillon, D. Skurnik, B. Picard and E. Denamur, *Nat. Rev. Microbiol*., **2010**, *8*, 207.
32. A. E. Stella, T. F. Lima, C. N. Moreira and E. M. N. De Paula, *Int. J. Microbiol*., **2020**, 2893027.
33. D. Jaroni, "SALMONELLA | Salmonella typhi", in "Encyclopedia of F. Microbiology", 2nd edition, 2014.
34. S. Panayidou, K. Georgiades, T. Christof, S. Tamana, V. J. Promponas and Y. Apidianakis, *Sci. Rep.*, **2020**, *10*, 9505.
35. https://microbiologyinfo.com/mueller-hinton-agar-mha-composition-principle-uses-and-preparation/